Available online at www.sciencedirect.com
ScienceDirect
International Journal of Heat and Mass Transfer 50 (2007) 292–302
International Journal of HEAT and MASS TRANSFER
www.elsevier.com/locate/ijhmt

Conduction through an assembly of spherical particles at low liquid contents

E.G. Youngs [a,*], A.R. Kacimov [b]

[a] Institute of Water and Environment, Cranfield University, Silsoe, Bedford MK45 4DT, England, United Kingdom
[b] Department of Soils, Water and Agricultural Engineering, P.O. Box 34, Al-Khod 123, Sultan Qaboos University, Oman

Received 4 August 2005
Available online 17 August 2006

Abstract

The steady-state conduction of heat through the solid phase of a porous material consisting of an assembly of simple cubic packed uniform spheres at low liquid contents with heat conducted from one sphere to the next through annular liquid lenses around the points of contact, is analysed in terms of Legendre polynomials assuming the liquid bridges to behave as isothermal hemispheres around point sources and sinks. The conductance of a sphere is approximately the same when the surface area of the hemisphere is the same as that of the liquid lens assumed to be an isothermal disc for which numerical results of isotherms are compared with the analytical results.

Keywords: Porous materials; Open- and close-packed spheres; Conductance; Effective conductivity; Laplace's equation; Analytical solutions

1. Introduction

Heat transfer in porous materials occurs both by conduction through the constituting solid, liquid and gaseous phases and by convection with the moving liquid and gas in the pore network. In unsaturated materials it is also affected by distillation between liquid islands where evaporisation and condensation occur [1]. In this paper we focus on the conduction of heat through the solid particles at low liquid contents, considering the three-dimensional flow between isolated lenses of liquid in the interstices. We consider steady conduction only that depends on the arrangement of solid particles and on the proportions of liquid and gas that fill the void space. It decreases with the liquid content since the conductivity of gases is generally negligible compared with that of liquids and solids.

The process has been studied extensively in work on the thermal behaviour of soils where effective conductivities of the multiphase system occurring in wet soils are used to describe the macroscopic flow. Hillel [2, p. 286] states that "the problem of expressing the overall thermal conductivity of a soil as a function of the specific conductivities and volume fractions of the soil's constituents is very intricate, as it involves the internal geometry of soil structure and the transmission of heat from particle to particle and from phase to phase". The detailed reproduction of the intricacy is commonly obviated in effective medium theories that consider the effective conductivity k_e of the bulk material. These originate from the Maxwell [3] and Bruggeman [4] approach that considers a single ellipsoidal particle embedded in a homogeneous medium. Mathematically the problem reduces to the three-dimensional refraction of an external field at the ellipsoid surface where the thermal conductivity changes from that of the medium to that of the particle. In soil physics, the effective conductivities as considered by de Vries [5,6] were developed from Burger's [7] equation for the electrical conductivity of a porous material that follows Maxwell's conceptualisation.

Models based on the Maxwell–Bruggeman approach work well when the liquid content is large so that the solid phase appears to be embedded in a matrix of the liquid

* Corresponding author. Tel.: +44 (0) 1525 863330; fax: +44 (0) 1525 863344/001.
E-mail addresses: e.g.youngs@cranfield.ac.uk (E.G. Youngs), anvar@squ.edu.om (A.R. Kacimov).

0017-9310/$ - see front matter © 2006 Elsevier Ltd. All rights reserved.
doi:10.1016/j.ijheatmasstransfer.2006.06.006

Nomenclature

a	radius of sphere (m)
G	conductance (W K^{-1})
$\vec{i}$	external (effective) thermal gradient in the porous medium (K m^{-1})
k	thermal conductivity of solid material (W m^{-1} K^{-1})
k_e	effective conductivity of the packing (W m^{-1} K^{-1})
q	strength of point sources and sinks (W)
Q	total heat conducted through one sphere (W)
(r,θ,ω)	spherical coordinates (m,–,–)
r_c	radius of isothermal caps (m)
r_d	radius of disc source and sink (m)
r_{hs}	radius of hemispherical source and sink (m)
S	surface area of an arbitrary isotherm (m^2)
t	fictitious time in particle tracking (s)
t_f	marching time in the Runge–Kutta algorithm (s)
T	temperature within sphere (K)
T_0	temperature of hemispherical sources modelling water lenses (K)
T_i	induced temperature (K)
T_{si}, T_{so}	temperature components due to point singularities (K)
V	volume confined by an arbitrary isotherm and adiabatic plane (m^3)
(x,y,z)	Cartesian coordinates (m)

phase. However, this is not the case in unsaturated soils where there is no liquid continuity so that heat flow is channelled through areas around contacting particles. Thus the de Vries analytical equation overestimates the thermal conductivity at low liquid contents while empirical formulae that give good estimates of the thermal conductivity at large liquid contents fail as the liquid content approaches zero. Chudnovskii [8] gives a comprehensive review and numerous experimental data for heat conduction at low water contents in soils and porous materials of different density, texture and mineralogy of solid particles.

As the liquid content in a porous material decreases, a liquid that wets the surface of the solid matrix withdraws into the interstices at the touching points of particles forming the porous material, and conduction takes place only through the solid particles between thermal contacts if the conductivity of the gaseous phase is small and can be neglected. The heat flow within the solid particles is obviously three-dimensional and this is not considered in the simple macroscopic one-dimensional theories, although it has been qualitatively depicted in the patterns of heat flow converging to and diverging from the contact zones in adjacent particles [8]. A more rigorous approach to the conduction problem must include this three-dimensional flow between the contact areas of neighbouring particles.

In the analysis of thermal contact problems [9], although the temperature field near the contact is not uniform, the two regions are considered to be semi-infinite and either the temperature is postulated to be uniform at infinity [10,11] or the thermal gradient to be constant [12]. The spatial behaviour of temperature results from this far-field condition and the conditions at the contacts which are considered to behave as point or line sinks or sources. These semi-unbounded regions differ from a finite particle in a porous material in which these conditions do not apply.

Modelling porous materials as an assembly of spheres has been used extensively in work on heat transport in such materials. Gemant [13] considered water located in lenses at the points of contact, but assumed one-dimensional flow through the sphere in calculating the soil's thermal conductivity. Gusarov et al. [14] and Siu and Lee [15] considered thermal contacts as either polar caps or necks connecting the neighbouring spheres. Their contiguous spheres constituted the elementary cells of a lattice forming the representative elementary volume for the macroscopic behaviour. Chen and Tien [16] assumed isotherms are normal to the direction of the macroscopic heat flow and obtained a formula for the conductance of a spherical packing. If the liquid is nonwetting, then droplets of liquid form in the porous matrix and heat flows through thermal contacts occurring as disc-shaped quasi-spherical zones of liquid between solid particles [18].

In order to investigate further the conduction of heat at small liquid contents in porous materials, we first consider the simplest system of an assembly of simple cubic open-packed spheres and consider the flow between the liquid lenses around the contact points assumed to be isothermal zones. It has not been possible to find an analytical solution to Laplace's equation that describes the flow within the spheres that was solved by Youngs [17] numerically for the analogous problem of water flow through porous aggregates when the larger pores surrounding the aggregates are full of air and the fluid flow is funnelled through small water lenses around the contact points. However, if we consider the points of contact to behave as point sources and sinks as was done by Avkhadiev and Kacimov [19], which is equivalent to assuming the areas of contact are approximately hemispherical, solutions are possible. In this paper we present this solution that describes the heat flow within the sphere and provides an insight into the microscopic behaviour in the solid phase. We also consider the situation of flow in a close-packed assembly of uniform spheres.

2. Open-packed uniform spheres

We consider the conduction of heat through an assembly of open-packed spheres of radius a and uniform conductivity k arranged as a lattice in a cubic packing

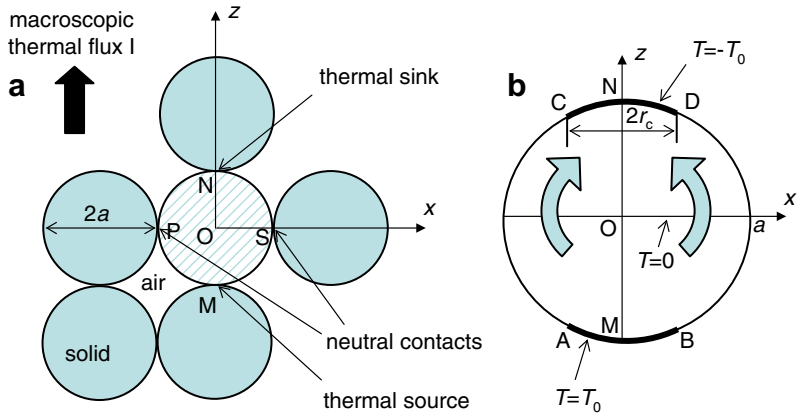

Fig. 1. Simple cubic open packing of spheres: (a) cross-section of an assembly and (b) of an elementary cell.

(Fig. 1a). An elementary cell of the lattice has three planes of symmetry and a coordination number of six so that each sphere touches six neighbours. The porosity of this packing is $1-\pi/6$. In the elementary cell of the lattice, heat is conducted from one sphere to another through contact zones AMB and CND shown in the plan view in Fig. 1b around the poles M, N, and at four positions P, S and two other contact points not shown around the equator. We neglect radiation heat transfer and the heat conduction from the solid surface to and from the gas phase because of the latter's small conductivity relative to k, and assume there is no convective flow of liquid and gas and no heat exchange due to evaporation and condensation from the liquid islands that form the contact zones.

In the simplest case the external temperature gradient i is perpendicular to one of the planes of symmetry (plane xOy in Fig. 1a) so that macroscopically heat flows parallel to the z-axis. Conduction of heat to or from the sphere MPNS is provided by the two spheres stacked just above and below through the zones of contact near the bottom M and top N. The four other neighboring spheres in the horizontal plane are thermally neutral.

We assume that zones of particle contact can be regarded as small isothermal caps of a radius r_c ($r_c \ll a$) as shown in Fig. 1b that depicts the xOz cross-section of the sphere. With temperatures measured relative to the average temperature of the sphere, the cap AMB is at temperature $T = T_0$ and the cap CND is at temperature $-T_0$. Due to symmetry the equatorial plane $z = 0$ is also an isotherm at temperature $T = 0$. The temperature distribution within the sphere is given by solutions of Laplace's equation subject to the given boundary conditions.

If we assume that the porous material behaves as a continuum consisting of solid spheres and interstitial space, then the one-dimensional macroscopic heat flux I is given by Fourier's law:

$$I = -k_e \frac{dT}{dz} = -k_e i \tag{1}$$

where k_e is the apparent macroscopic conductivity of the two-phase system. The apparent temperature gradient T_0/a over one particle is trivially expressed through the macroscopic thermal gradient i. Microscopically we are concerned with the temperature distribution within individual spheres.

3. Weber disc limit

For very large sphere radii and small cap radii the flow between the poles of a sphere in an open-packed assembly approaches that of Weber's classical problem of the field due to an electrified disc in an infinite medium. Then the temperature field around a disc of radius r_d is given by Carslaw and Jaeger [20]:

$$\begin{aligned} T &= \frac{2T_0}{\pi}\int_0^a e^{-\lambda z} J_0(\lambda r)\sin(\lambda a)\frac{d\lambda}{\lambda} \\ &= \frac{2T_0}{\pi}\arcsin\frac{2r_d}{\sqrt{(r-r_d)^2+z^2}+\sqrt{(r+r_d)^2+z^2}} \end{aligned} \tag{2}$$

in cylindrical coordinates, where J_0 is the Bessel function of the first kind and $T = T_0$ on the disc's surface $r < r_d$, $z = 0$, $\partial T/\partial z = 0$ at $r > r_d$, $z = 0$, and $T \to 0$ at r, $z \to \infty$. In the analogous groundwater situation it has been shown that equipotentials (analogous to the isotherms) are spheroids and stream surfaces are hyperboloids [21]. The total heat Q conducted from the disc is given by

$$Q = 4kr_d T_0 \tag{3}$$

Scaling arguments were used in [17] to show that (3) describes the flow between small polar caps of radius r_c ($\approx r_d$) in spheres of any radius a. The conductance G of any sphere of radius a is thus $Q/2T_0 = 2kr_c$, giving the effective conductivity of the assembly of open-packed spheres as

$$k_e = kr_c/a \tag{4}$$

4. Point source and sink solution

In order to obtain an analytical closed-form solution to Laplace's equation

$$\Delta T = 0 \tag{5}$$

for the temperature distribution within a sphere of radius a in an open-packed assembly, we assume flow from a point source of strength q located at point M, $z=-a$, $x=0$, $y=0$ to a sink of strength $-q$ at N, $z=a$, $x=0$, $y=0$ (Fig. 1b). On the surface of the sphere

$$\frac{\partial T}{\partial r} = 0 \tag{6}$$

at $r=a$ except at points M and N. The polar sources and sinks around M and N coincide with the isotherms

$$T = \pm T_0 \tag{7}$$

and become practically hemispherical in the vicinity of M and N. The harmonic function T can be represented as the sum

$$T = T_{so} + T_{si} + T_i \tag{8}$$

where T_{so} and T_{si} are the temperature fields generated by the source and sink. These harmonic functions using the dimensionless variables $(X, Y, Z, R) = (x, y, z, r)/a$ are [21]:

$$\begin{aligned} T_{so} &= \frac{q}{4\pi ka}\frac{1}{\sqrt{(Z+1)^2+X^2+Y^2}}, \\ T_{si} &= -\frac{q}{4\pi ka}\frac{1}{\sqrt{(Z-1)^2+X^2+Y^2}} \end{aligned} \tag{9}$$

or in spherical coordinates

$$\begin{aligned} T_{so} &= \frac{q}{4\pi ka}\frac{1}{\sqrt{R^2+1+2R\cos\theta}}, \\ T_{si} &= -\frac{q}{4\pi ka}\frac{1}{\sqrt{R^2+1-2R\cos\theta}} \end{aligned} \tag{10}$$

The third function T_i in (8) is the induced temperature, which is also harmonic and obtained from the no-flux boundary condition on the sphere's surface

$$\frac{\partial T_i}{\partial R} = -\frac{\partial T_{so}}{\partial R} - \frac{\partial T_{si}}{\partial R} \quad \text{at } R=1 \tag{11}$$

We search this function in the general form as a multipolar series expansion [22]

$$T_i = \sum_{n=0}^{n=\infty} b_n R^n P_n(\cos\theta) \tag{12}$$

where P_n are Legendre polynomials and b_n are expansion coefficients. These coefficients are found by differentiating (10) and (12) and using (11) yielding

$$\sum_{n=0}^{n=\infty} n b_n P_n(\cos\theta) = \frac{q}{8\sqrt{2}\pi ka}\left[\frac{1}{\sqrt{1+\cos\theta}} - \frac{1}{\sqrt{1-\cos\theta}}\right] \tag{13}$$

The coefficients b_n are then found from formula (4.7.2) in [23] by expanding the right hand side of (13) into the Legendre polynomial series, giving

$$\begin{aligned} b_n = \frac{(2n+1)q}{16\pi\sqrt{2}nka}\Bigg[&\int_0^\pi P_n(\cos\theta)\frac{\sin\theta}{\sqrt{1+\cos\theta}}\mathrm{d}\theta \\ &- \int_0^\pi P_n(\cos\theta)\frac{\sin\theta}{\sqrt{1-\cos\theta}}\mathrm{d}\theta\Bigg] \end{aligned} \tag{14}$$

From formula 2.7.11 in [22] the first integral in (14) is equal to $2\sqrt{2}n/(2n-1)(2n+1)$, and since $P_n(x) = (-1)^n P_n(-x)$ the second integral is equal to the first multiplied by $(-1)^n$, so that

$$\begin{aligned} &b_0 = b_2 = b_4 = \cdots = 0, \quad b_{2n-1} = -\frac{q}{4\pi(2n-1)ka}, \\ &n = 1, 2, 3, \ldots \end{aligned} \tag{15}$$

Using these values of b_n, T_i can be calculated from (12) and the distribution of T obtained from (8) with T_{so} and T_{si} given by (10). Alternatively, using the Mehler–Dirichlet integral representation for the Legendre polynomials (formula (4.4.4) in [22]) gives

$$\begin{aligned} T_i = -\frac{\sqrt{2}q}{4\pi^2 ka}\Bigg[&\int_0^\theta \cos(\psi/2)\sum_{n=1}^{\infty}\frac{R^{2n-1}\cos(2n-1)\psi}{2n-1}\frac{\mathrm{d}\psi}{\sqrt{\cos\psi-\cos\theta}} \\ &- \int_0^\theta \sin(\psi/2)\sum_{n=1}^{\infty}\frac{R^{2n-1}\sin(2n-1)\psi}{2n-1}\frac{\mathrm{d}\psi}{\sqrt{\cos\psi-\cos\theta}}\Bigg] \end{aligned} \tag{16}$$

The second integral of (16) can be summed according to the first formula 5.4.9.16 in [23]. Unfortunately, we found the second formula 5.4.9.16 in [23] for the first integral to be incorrect so we used Eq. (1.448.4) in [24]. Finally, the induced temperature is

$$\begin{aligned} T_i = &-\frac{\sqrt{2}q}{16\pi^2 ka} \\ &\times\Bigg[\int_0^\theta \frac{\cos(\psi/2)\log[(1+2R\cos\psi+R^2)/(1-2R\cos\psi+R^2)]\mathrm{d}\psi}{\sqrt{\cos\psi-\cos\theta}} \\ &- \int_0^\theta \frac{2\sin(\psi/2)\arctan[(2R\sin\psi)/(1-R^2)]\mathrm{d}\psi}{\sqrt{\cos\psi-\cos\theta}}\Bigg] \end{aligned} \tag{17}$$

Fig. 2 shows a plot of the isotherms in the sphere calculated for $q/ka = 1$.

The total heat being conducted through the sphere is

$$Q = -\int_0^{2\pi}\int_0^1 \left(\frac{\partial T}{\partial Z}\right)_{z=0} \rho\mathrm{d}\rho\mathrm{d}\omega \tag{18}$$

where $(\partial T/\partial Z)_{z=0}$ is the equatorial value in the plane $Z=0$ ($\theta = \pi/2$). Differentiating (8) and integrating (18) we obtain

$$Q = q\left[1 - \frac{\sqrt{2}}{2} + \sum_{n=0}^{\infty}\frac{P_{2n}(0)}{4n+4}\right] = 0.5q \tag{19}$$

as it should be.

The isotherms are the same as if they were substituted by surfaces maintained at the same uniform temperature. Near the poles they become approximately hemispherical with a radius $r_{hs}(T) = aR_{hs}(T) = a\theta_{T,1}$ where $\theta_{T,1}$ is the value of θ where the temperature is T on the surface $R=1$. The conductance G of the sphere between two such

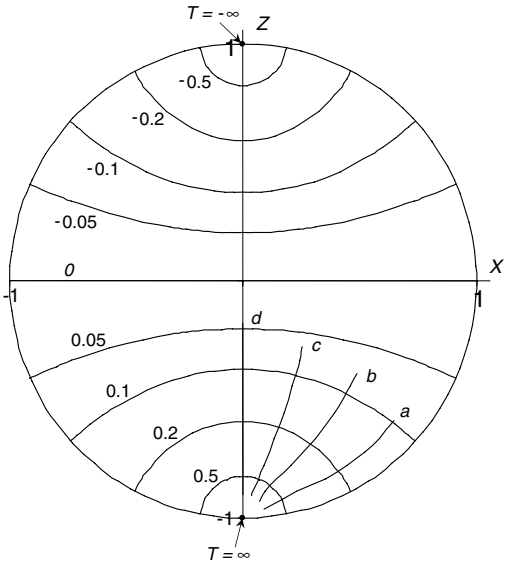

Fig. 2. The temperature distribution for heat flow between a point source and a point sink at opposite poles of a sphere. Isotherms are shown for $q/ka = 1$. Curves a–f are "streamlines".

isothermal surfaces maintained at T_0 and $-T_0$ is $Q/2T_0$. The effective conductivity of an assembly of such open-packed spheres is $G(r_{\mathrm{hs}})/2a$.

Streamlines, which are a most important part of the solutions of the analogous problems of water flow in soils and liquid flow in porous materials in general, are not often derived in heat flow problems. Nevertheless, in the thermal situation these curves provide a good insight into the funnelling features around thermal contact zones and are often shown qualitatively (see, for example, [8–10,12]). These can be plotted in a plane (ρ, z) based on the known particle tracking algorithm, which follows from the solution of the system of ordinary differential equations

$$z'(t) = v_z(\rho, z), \quad \rho'(t) = v_\rho(\rho, z) \tag{20}$$

In (20) we follow Fourier and treat conduction as if it were a phenomenon of continuous flow of an imponderable "fluid" without regard to the underlying microstructure of the solid phase continuum. Correspondingly, the thermal gradient components $v_z = -k\partial T/\partial z$, $v_\rho = -k\partial T/\partial\rho$ in (20) are related to a fictitious "fluid" particle with Lagrangian coordinates z, ρ. The particle is kinematically advected in the sphere with a fictitious "time" t along a fictitious "streamline" (which in electrostatics Faraday called a "curved line of inductive action" and Lord Kelvin called it a "force line"). In seepage problems [21] the movement of fluid particles is real and $\vec{v}$ is divided by porosity to arrive at the linear average velocity.

The derivatives in (20) are calculated routinely by computer packages, for example by **D** of *Mathematica*. Then (20) is solved by **NDSolve** as the Cauchy problem with initial values z_0, ρ_0 with time marching, $0 < t < t_{\mathrm{f}}$ where t_{f} is the limit when a marked particle reaches the sink at point N in Fig. 1. Curves a–d in Fig. 2 show the streamlines originating from the isotherm $T = 1.0$ and tracked up to $t = 1.4$, illustrating the greater distance traversed in a given time by particles in the centre of the sphere compared to those near the circumference.

5. Arbitrary oriented external gradient

In the above we have considered flow caused by an external gradient normal to the equatorial plane between poles. The general case is when this gradient is inclined so that flow takes place also through the points of contact around the equator.

We consider an external gradient $\vec{i}$ having three arbitrary components i_x, i_y and i_z. The y-component of $\vec{i}$ can be made zero by rotating the coordinate system xyz, so that without any loss of generality we can assume that $i_x > 0$, $i_z > 0$, $i_y = 0$. Then two of the six contact points for each sphere in Fig. 1 are still thermally inactive and heat flows from two sources at points M and P with strengths q_z and q_x respectively to two sinks at points N and S with strengths $-q_z$ and $-q_x$.

The temperature field generated by the combined action of two source–sink pairs is the sum of the two solutions already obtained for $i_x = 0$ but with the difference that for the source–sink pair at P and S we have to permute $z \to x$ and change θ to $\pi/2 - \theta$. Thus we have

$$T = T_{\mathrm{zso}} + T_{\mathrm{zsi}} + T_{\mathrm{zi}} + T_{\mathrm{xso}} + T_{\mathrm{xsi}} + T_{\mathrm{xi}} \tag{21}$$

$$T_{\mathrm{zso}} = \frac{q_z}{4\pi ka}\frac{1}{\sqrt{(Z+1)^2 + X^2 + Y^2}},$$

$$T_{\mathrm{zsi}} = -\frac{q_z}{4\pi ka}\frac{1}{\sqrt{(Z-1)^2 + X^2 + Y^2}},$$

$$T_{\mathrm{xso}} = \frac{q_x}{4\pi ka}\frac{1}{\sqrt{(X+1)^2 + Y^2 + Z^2}},$$

$$T_{\mathrm{xsi}} = -\frac{q_x}{4\pi ka}\frac{1}{\sqrt{(X-1)^2 + Y^2 + Z^2}},$$

$$T_{\mathrm{zi}} = \sum_{n=0}^{n=\infty} b_n R^n P_n(\cos\theta),$$

$$T_{\mathrm{xi}} = \sum_{n=0}^{n=\infty} b_n R^n P_n(\cos(\pi/2 - \theta))$$

with b_n calculated by (15).

The distribution of T in a cross-section $Y = 0$ were computed from (21) for the case of $q_x/ka = q_z/ka = 1$, that is, for the orientation of the external field at 45° to the x and z lattice axes which characterises the ambient field most deflected with respect to the axially-oriented case studied in Section 4. This situation is illustrated in Fig. 3 and isotherms are plotted in Fig. 4. There is obviously a no-flow plane $Z = X$ while the plane $Z = -X$ is an isotherm. While the contours for $T = 0$, $T = \pm 0.1$ and $T = \pm 0.2$ are single-connected, $T = \pm 0.3$ and $T = \pm 0.5$ are double-connected.

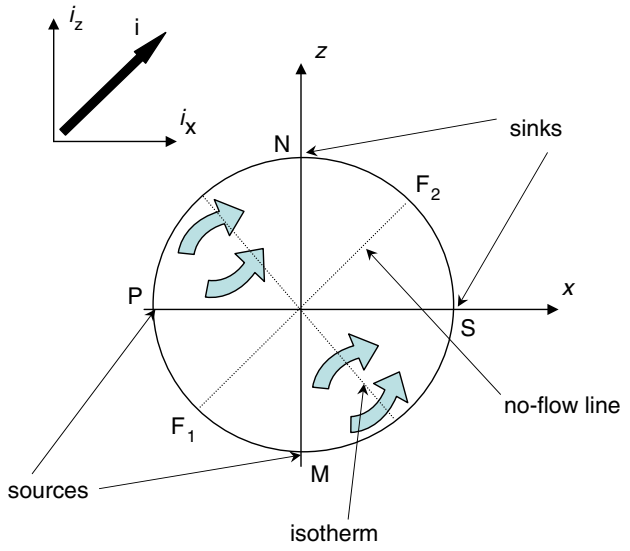

Fig. 3. Heat flow due to an oriented external thermal gradient in a cross-section of a sphere.

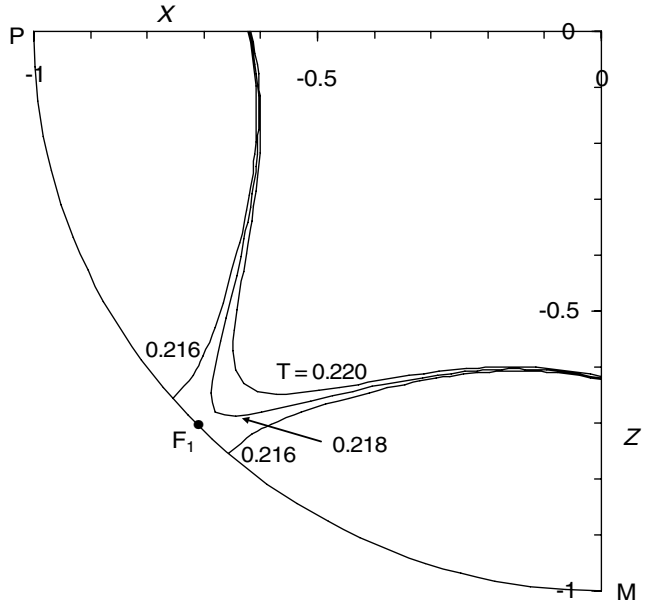

Fig. 5. The isotherms near the critical point F_1.

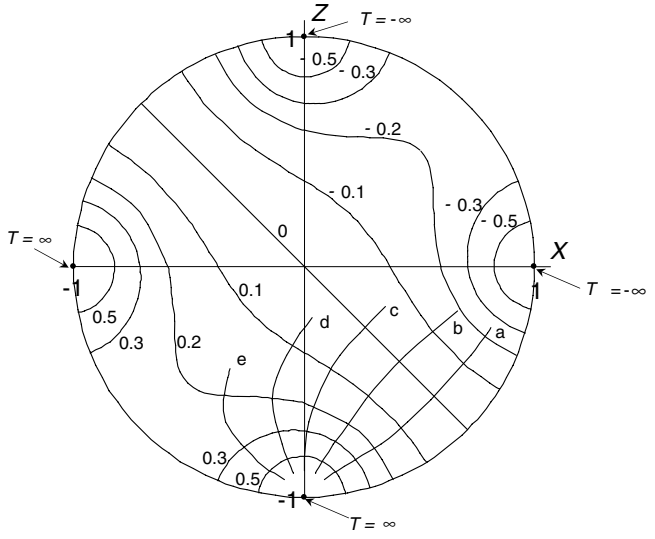

Fig. 4. The temperature distribution for heat flow between point sources and sinks in the sphere due to an external thermal gradient oriented at π/4 to the polar axis. (a) Isotherms are shown for $q_x/ka = q_z/ka = 1$; curves a–f are "streamlines".

The latter consist of two isotherms enclosing the two sources and sinks. With the increase of T these isotherms become more hemispherical. Curves a–e show "streamlines" plotted by particle tracking according to (20) from a small sphere of radius $R = 0.1$ surrounding point M with a marching time $t_f = 1.4$. Streamlines a and b passed two-thirds of the whole distance between the source and sink while trajectories d and e did not reach even the isothermal surface $T = 0$ during this time lapse.

To understand better the heat flow topology Fig. 5 shows magnified the zone near the two sources with isotherms $T = 0.216$, 0.218, 0.220. The first two contours are single-connected and they converge to a critical point F_1. At this point two "streamlines" coming from the sources "impinge" on the no-flow plane $x = z$ and the "velocity" (∇T) there is zero. Obviously, for the half of the sphere that is above the plane $z = -x$ the picture is symmetrical and F_2 (Fig. 3) is the second critical point.

Again we note that around the poles the isotherms approximate to hemispheres and these are the same as if they were substituted by surfaces maintained at the same uniform temperature. In this multi-pole situation the values of $\theta_{T,1}$ either side of the pole differ by a small amount so we take an average value to obtain a value of $r_{hs}(T)$ which was found to be the same as the value obtained for the single-pole situation. The conductance then between the two sources and the two sinks on the sphere is

$$G'(r_{hs}) = 2Q/2T_0 = Q/T_0 = 2G(r_{hs}) \tag{22}$$

that is, double that found for the previous situation of flow between only two poles. The macroscopic gradient for the flow on the assembly of spheres in this case is $2T_0/\sqrt{2}a$. The total flow over unit cross-section is $2Q/4\sqrt{2}a^2$ so that the effective conductivity is

$$k_e = Q/4T_0a = G(r_{hs})/2a \tag{23}$$

the same value as obtained when the flow is between opposite polar caps. This thus confirms that the orientation of the gradient causing transport in an assemble of open-packed spheres does not affect the macroscopic flow which is therefore isotropic.

6. Close-packed uniform spheres

We now consider the more complicated case of an assembly of tetrahedral close-packed uniform spheres of

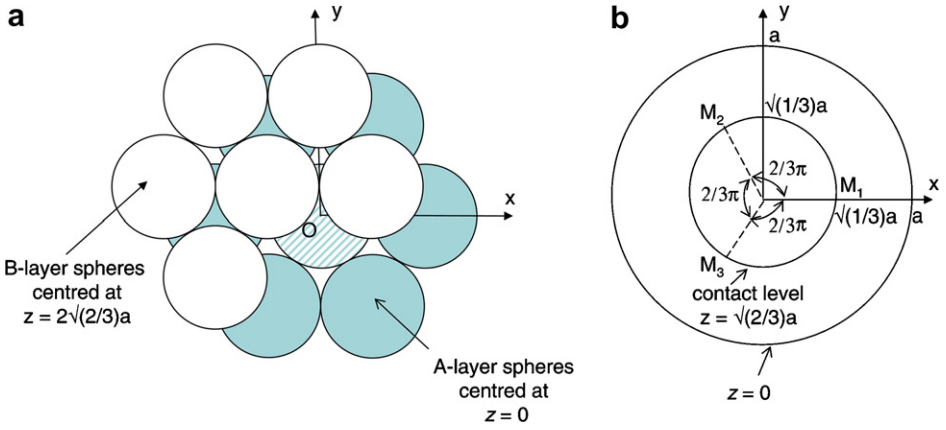

Fig. 6. Tetrahedral close packing of spheres packing of spheres.

radius a. In this situation the spheres are arranged in a repeated layered hexagonal pattern (Fig. 6a), the particles of one layer falling between those of the next forming tetrahedral grouping of the spheres with a spacing between layers of $2\sqrt{2/3}a$. The coordination number of an elementary cell in this case is twelve with each sphere touching twelve neighbours. The porosity of this packing is $1-\pi/(3\sqrt{2})$. We consider the hatched sphere in Fig. 6a located at the origin O in the A-layer, all sphere centres of which are located in the xOy plane. Fig. 6b shows the plan sections of this sphere in the equatorial plane $z=0$ and through the three contact points M_1, M_2 and M_3 located on a radius $\sqrt{1/3}a$ in the plane $z=\sqrt{2/3}a$. Six neighbours contact the hatched sphere in the plane $z=0$, and there are three contact points on a radius $\sqrt{1/3}a$ in the plane $z=-\sqrt{2/3}a$ on the layer below that is a reflection of the B-layer.

We consider the simplest orientation of the ambient thermal gradient along the z-axis. It implies that the six neighbouring spheres on the equator in the plane xOy are thermally neutral. Heat enters the cell from three point sources in the plain $z=-\sqrt{2/3}a$ and leaves through M_1, M_2 and M_3 in Fig. 6b. In our spherical coordinates the azimuthal angles of M_1, M_2 and M_3 are $\omega_1=0$, $\omega_2=2/3\pi$ and $\omega_3=4/3\pi$ correspondingly. The latitude coordinate of all these points is $\theta_{1-3}=\arccos\sqrt{2/3}$. Therefore, our temperature field is symmetrical about the xOy plane and will retain only one set of spherical harmonics in the expansion below. The three sources supplying heat into the cell have the same $\omega_1,\omega_2,\omega_3$ but $\theta_{1-3}=\pi-\arccos\sqrt{2/3}$. If we assume that the total heat flow through the sphere is Q then the intensity of each sink and source is $q=\pm Q/3$.

Similar to the case of open packing studied in the previous sections, we search for a harmonic function that is a sum of three sources and three sinks of a given form and one induced temperature $T_{\rm i}$ which is to be determined from the solution of the Neumann boundary-value problem:

$$T=\sum_{l=1}^{3}T_{l\rm so}+\sum_{l=1}^{3}T_{l\rm si}+T_{\rm i} \tag{24}$$

$$T_{l\rm si}=-\frac{q}{4\pi ka}\frac{1}{\sqrt{(Z-\sqrt{2/3})^2+(X-X_l)^2+(Y-Y_l)^2}},$$

$$T_{l\rm so}=\frac{q}{4\pi ka}\frac{1}{\sqrt{(Z+\sqrt{2/3})^2+(X-X_l)^2+(Y-Y_l)^2}}$$

$$X_l=1/\sqrt{3}\cos[(l-1)2\pi/3],$$

$$Y_l=1/\sqrt{3}\sin[(l-1)2\pi/3],\quad l=1,2,3$$

Transforming the singularities in (24) to spherical coordinates for the sinks

$$T_{1\rm si}=-\frac{q}{4\pi}\frac{1}{\sqrt{R^2+1-2R\sqrt{2/3}\cos\theta-2R\sqrt{1/3}\sin\theta\cos\omega}}$$

$$T_{2\rm si}=-\frac{q}{4\pi}\frac{1}{\sqrt{R^2+1-2R\sqrt{2/3}\cos\theta+R\sqrt{1/3}\sin\theta\cos\omega-R/2\sin\theta\sin\omega}}$$

$$T_{3\rm si}=-\frac{q}{4\pi}\frac{1}{\sqrt{R^2+1-2R\sqrt{2/3}\cos\theta+R\sqrt{1/3}\sin\theta\cos\omega+R/2\sin\theta\sin\omega}} \tag{25}$$

In (24) and (25) we use the dimensionless variables $(X,Y,Z,R)=(x,y,z,r)/a$ as before. For the three sources feeding our elementary cell (25) should be changed with $q\to -q$ and $-2R\sqrt{2/3}\cos\theta\to 2R\sqrt{2/3}\cos\theta$.

Now the induced temperature depends on the longitude, i.e. our problem is genuinely three dimensional. Consequently, we search $T_{\rm i}$ in the form of a double series

$$T_{\rm i}=\sum_{m=0}^{\infty}\sum_{n}^{\infty}b_{n,m}R^nP_n^m(\cos\theta)\cos[m\omega] \tag{26}$$

where $n\geqslant m$ and $P_n^m(\cos\theta)$ are the Legendre functions. On the sphere surface $R=1$ the induced temperature satisfies the no-flow condition

$$\frac{\partial T_{\rm i}}{\partial R}=-\sum_{l=1}^{3}\frac{\partial T_{l\rm so}}{\partial R}-\sum_{l=1}^{3}\frac{\partial T_{l\rm si}}{\partial R} \tag{27}$$

everywhere except at the six point singularities. In (27) we calculated the derivatives. For example, for the first term on the right hand side from (24)

$$\frac{\partial T_{lsi}}{\partial R} = \frac{q}{16\pi\sqrt{2}} \frac{1}{\sqrt{1-\sqrt{2/3}\cos\theta - \sqrt{1/3}\sin\theta\cos\omega}} \quad (28)$$

The expansion coefficients $b_{n,m}$ are determined by double integration [24]:

$$b_{n,m} = -\frac{e_m}{n}\frac{2n+1}{4\pi}\frac{(n-m)!}{(n+m)!} \times \int_0^{2\pi} d\omega \int_0^{\pi} P_n^m(\cos\theta)\sin\theta\left(\sum_{l=1}^{3}\frac{\partial T_{lso}}{\partial R} + \sum_{l=1}^{3}\frac{\partial T_{lsi}}{\partial R}\right)d\theta \quad (29)$$

where $e_0 = 1$ and $e_m = 2$ for all other m.

Eq. (29) formally gives us the coefficients required to obtain the temperature distribution from Eq. (24). However, we were unable to do the analytical integration for $b_{n,m}$ and series conversion, and formidable problems which could not be overcome, were found in attempting to obtain values by numerical integration.

7. Disc sources and sinks

It is of interest to examine how the analytical solutions to the conduction problem considering flow between point sources and sinks on the sphere's surface that approximate to hemispherical sources and sinks, compare with results of the more practical situation of disc sources and sinks that occur, for example in the form of isothermal liquid menisci around contact points.

The temperature at a radial distance r resulting from a point source of strength q emitting into an infinite conducting material is

$$T = q/4\pi kr \quad (30)$$

so that for a hemispherical source of radius r_{hs} bounded by an isothermal hemisphere, maintained at a temperature T_0, and a plane passing through the hemisphere's centre (adiabatic everywhere but the equatorial circle of the sphere) the flow of heat is

$$Q_{hs} = q/2 = 2\pi kT_0 r_{hs} \quad (31)$$

The corresponding expressions for a flat disc of radius r_d are given by (2) and (3), so that $Q_{hs}/Q_d = \pi/2$ for $r_{hs} = r_d$. For $Q_{hs} = Q_d$, $r_{hs}/r_d = 2/\pi$. The isotherms for this situation are compared in Fig. 7 for $r_d = 1.0$ when $r_{hs} = 2/\pi$. It is seen that they are in fair agreement for $r > 2.0$.

For the situation of flow between a hemispherical source and a hemispherical sink at temperatures T_0 and $-T_0$ on opposite boundaries of a semi-infinite conducting slab with adiabatic faces, solution of Laplace's equation by the method of images results in

$$Q_{hs} = 2\pi kT_0 r_{hs}/(1-(r_{hs}/D)\log(2)) \quad (32)$$

for small values of r_{hs}/D, where $2D$ is the thickness of the slab. The corresponding solution of the mixed boundary-value problem for the flow between two opposite discs at

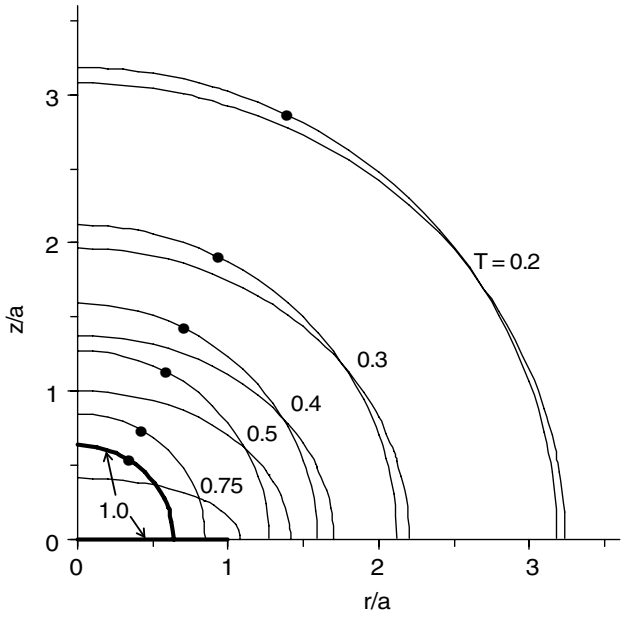

Fig. 7. Isotherms due to heat flow into a semi-infinite medium with zero temperature at infinity from a disc of unit radius at unit temperature (unmarked curves) and from a hemisphere with a radius of $2/\pi$ (marked by dots).

temperatures T_0 and $-T_0$ was given by Kliot–Dashinkii [26]. It was found there that the solution fitted the equation

$$Q_d = 4kT_0 r_d(1 + 0.88255R_d + 0.77889R_d^2 - 0.07785R_d^3 - 0.74408R_d^4 + 0.06752R_d^5 + 1.40148R_d^6) \quad (33)$$

to within 0.2% for $R_d < 2/3$, where $R_d = r_d/D$.

The relationship between the conductance $G = Q/2T_0$ and the radius of the disc, given in terms of the dimensionless variables G/kD and r_d/D, is shown in Fig. 8 where it is

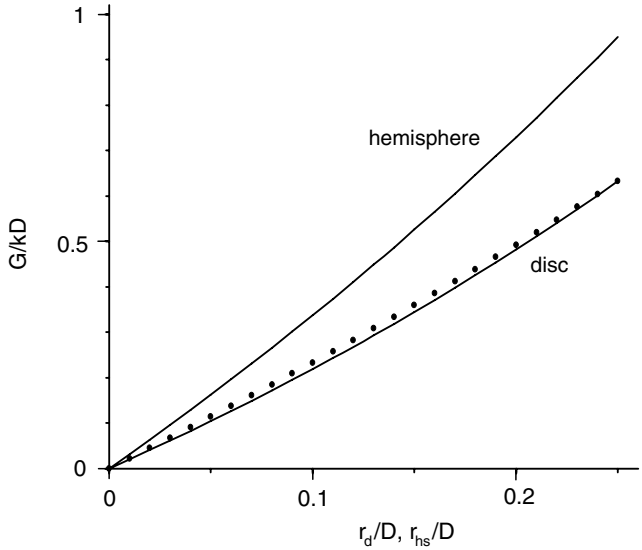

Fig. 8. The dimensionless conductance G/kD of a slab for heat flow between opposite pairs of discs and hemispheres plotted against the dimensionless radius of the discs r_d/D and hemispheres r_{hs}/D. The dots show values of the conductance of the discs if replaced by hemispheres with equal surface areas.

compared with Eq. (32) for a hemispherical source that gives a larger conductance for the same radius.

The complexity of solving the mixed boundary-value problem, as tackled in [25], was avoided by Das and Sadhal [27] by considering a constant-flux thermal contact zone in an infinite domain with a uniform induced flux at infinity. In an analogous infiltration problem Youngs et al. [28] also considered a constant-flux approximation to the physically uniform potential on the disc. For $r_{hs} = r_d$ the ratio $Q_{hs}/Q_d = \pi/2 = 1.571$ for $r_{hs}/D = r_d/D = 0$, increasing to 1.899 at $r_{hs}/D = r_d/D = 0.5$.

For an open-packed assembly of uniform spheres, the conductance of a sphere between a small hemispherical source and a small hemispherical sink on opposite poles is given from Eqs. (8), (10) and (12), and that between a small disc source and sink is given from Weber's formula as $2kr_d$. The relationships between the conductances for the two cases and the radius of the source are compared in Fig. 9, showing the larger conductance for the hemispherical source of the same radius.

In the groundwater situation of seepage from surface sources to a water-bearing permeable substratum, the surface source is often replaced by an equivalent cylindrical or spherical source of equal surface area. For the extreme case of a semi-infinite conducting material corresponding to the limit of an infinite sphere radius in our lattice, the analysis of Polya and Szego [29] gives two isoperimetric bounds for the heat flow Q conducted from a single isothermal surface at temperature $T = T_0$ to infinity. Although literally "isoperimetric estimates" mean comparisons of figures of equal perimeter, it is understood these estimates as bounding an integral physical property (e.g. electrostatic capacity), which is difficult to measure, by another property (e.g. volume or area), which can be relatively easily measured.

The Poincare–Faber–Szego [29] theorem states that

$$Q \geqslant 2\pi k T_0 \left(\frac{3V}{2\pi}\right)^{1/3} \tag{34}$$

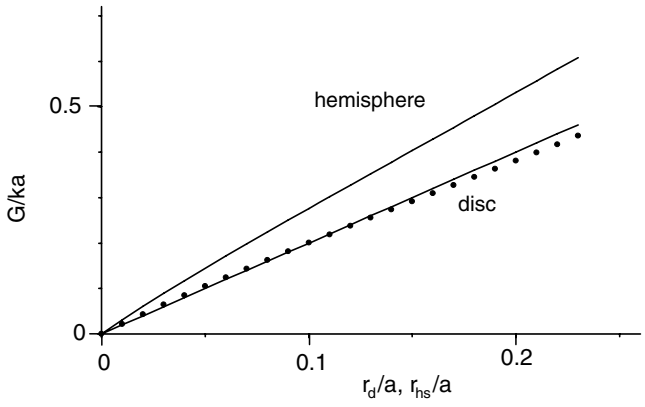

Fig. 9. The dimensionless conductance G/ka of a sphere for heat flow between opposite pairs of polar discs and hemispheres plotted against the dimensionless radius of the discs r_d/a and hemispheres r_{hs}/a. The dots show values of the conductance of the discs if replaced by hemispheres with equal surface areas.

where V is the volume confined by the surface and an adiabatic plane, on which this surface is based. The minimum of Q for a given V is attained with a hemisphere of radius r_{hs} so that from (34) $Q_{min} = Q_{hs} = 2\pi k T_0 r_{hs}$. The lower bound of Q for an arbitrary isotherm is also based on its surface area S. It is reported in [30] that $Q > Q_d$, so that the Weber disc gives minimal heat flow for a given S. Recent developments on isoperimetric inequalities for Q are discussed by Crasta et al. [30] for unbounded domains or, assuming shape symmetry of the generating isothermal source, for semi-infinite domains. It would be challenging to extend this analysis and to find out how the hemisphere and disc optimal shapes transform for finite regions such as in the problem of conduction in spheres between thermal contact zones.

With a hemispherical source of the same surface area as the disc in the unbounded situation, that is $r_{hs} = r_d/\sqrt{2}$, the ratio of the flow rates for the same potential difference is

$$\frac{Q_{hs}}{Q_d} = \frac{G_{hs}}{G_d} = \frac{\pi}{2\sqrt{2}} \approx 1.11 \tag{35}$$

The good approximation obtained for the conductance of a disc source and sink using an equivalent hemispherical source and sink of equal surface area in the bounded situation of the conduction in a slab and a sphere, is shown in Figs. 8 and 9.

8. Comparison with numerical results

It is of interest to compare the temperature distribution in the sphere between polar caps with that given by (8) for heat flow between isothermal surfaces with the same

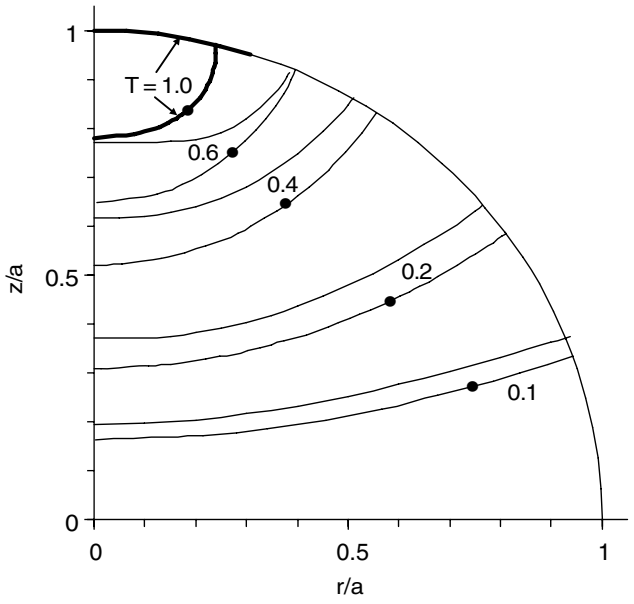

Fig. 10. Comparison of isotherms for flow between a polar disc source at $T = 1$ and a polar sink at $T = -1$ of radius $r_d = 0.314a$ obtained by finite difference calculations (unmarked curves) and analytical results for a hemispherical source at $T = 1$ and sink at $T = -1$ of radius $r_{hs} = 0.222a$ (marked by dots).

surface area around a point source and sink that approximate to hemispheres. Such a comparison is shown in Fig. 10 in which the numerical solution of Youngs [17] for two polar isothermal caps $R = 1$, $\pm\pi/2 - \pi/10 < \theta < \pm\pi/2$ kept at temperatures $T = \pm 1$ is compared with the analytical temperature distribution for a hemispherical source and sink giving the same flow rate. The numerical solution was obtained using the over-relaxation finite difference method. The flow rate for this size disc was $Q_d/ka = 1.216$ which was used in our analytical sink–source solution. It is seen that even for this large disc the coincidence of the two temperature distributions are reasonably close in the central region of the sphere.

9. Discussion

In this study we have considered the steady-state heat conduction through an assembly of uniformly packed spheres in order to understand more fully the thermal regime in porous materials at low liquid contents when the liquid is held in interstices between the particles at contact points. It is assumed that the conductivity of the gas phase is small relative to that of the material of the spheres, and that the liquid lenses act as thermal contacts between the particles. It is also assumed that there is no heat exchange due to evaporation and condensation at the liquid islands that occurs with thermally enhanced vapour transport particularly at high temperatures [1,31]. For an open-packed assembly of uniform spheres, this results in the conductance of a sphere being given by Weber's formula for flow from a disc into a semi-infinite medium. However, a full analytical treatment of the flow regime within the sphere has not been possible for this situation. Instead we have supposed that the contact points can be replaced by point sources and sinks surrounded by approximate hemispherical isotherms that replace the disc sources and sinks in the actual problem. This has allowed an explicit analytical solution to the problem in terms of Legendre polynomials, giving the three-dimensional pattern of isotherms within a sphere and illustrating the complexity of calculating thermal conductivities of porous materials.

In considerations of the thermal regime in soils and porous materials in general the macroscopic behaviour is obtained by using an equivalent or effective conductivity that depends on the liquid content. Our analysis of the temperature distribution in a sphere within a simple cubic packing of spheres at small liquid contents gives the conductance of a sphere, and hence the effective conductivity, in terms of the size of the annular water lenses in the interstices between particles relative to the sphere's radius. The liquid content w due to the lenses held by surface tension forces in the interstices between spheres is [32]:

$$w = \frac{3\pi}{4}(\sec\alpha - 1)^2\left[1 - \left(\frac{\pi}{2} - \alpha\right)\tan\alpha\right] \tag{36}$$

where α is the angle subtended at the origin of the sphere by the circular lens of liquid. For a simple cubic packing the

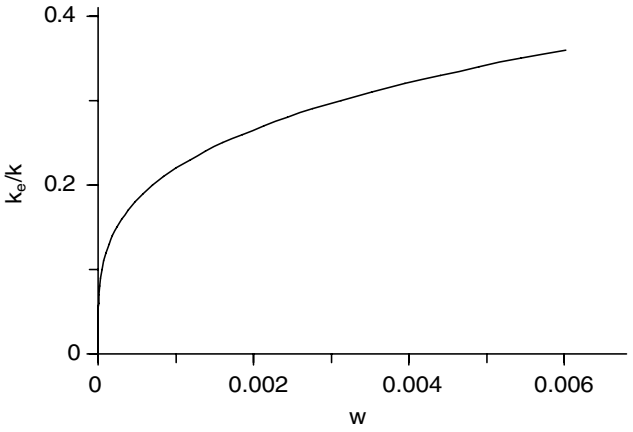

Fig. 11. The effective conductivity as a fraction of the conductivity of the solid particle k_e/k plotted against the liquid content w for a simple cubic close packing of uniform spheres.

effective conductivity is given by $G/2a$, so that with the conductance G given by Weber's formula as $G = 2kr_c$, $k_e = kr_c/a = k\alpha$, and (36) gives the relationship between the effective conductivity and the liquid content shown in Fig. 11. The form of this predicted behaviour agrees with measurements of the effective thermal conductivity of porous materials [7,33,34].

The analysis given here also applies to the conduction of electricity through spherical particles of a porous materials and to the flow of fluids through porous aggregates. In the latter case the flow velocity is of special interest, especially in the consideration of the movement of solutes [17].

References

[1] J.R. Philip, D.A. de Vries, Moisture movement in porous materials under temperature gradients, Trans. Am. Geophys. Union 38 (1957) 222–232.
[2] D. Hillel, Fundamentals of Soil Physics, Academic Press, San Diego, 1980.
[3] J.C. MaxwellA Treatise on Electricity and Magnetism, vol. 1, Oxford University Press, Oxford, 1998.
[4] D.A.G. Bruggeman, Berechnung verschiedener physikalischer Konstanten von heterogenen Substanzen. I.Dielektrizitatskonstanten und Leitfahigkeiten der Mischkorper ausisotropen Substanzen, Ann. Phys. (Leipzig) 24 (1935) 636–679.
[5] D.A. de Vries, Het warmtegeleidingsvermogem van grond. Thesis Meded. Landbouwhogeschool, Wageningen, 52 (1952), 1–73.
[6] D.A. de Vries, Thermal properties of soils, in: W.R. van Wijk (Ed.), Physics of Plant Environment, North-Holland, Amsterdam, 1963, pp. 210–235.
[7] H.C. Burger, Das Leitvermögen verdünnter mischkristallfreier Lösungen, Phys. Z. 20 (1915) 73–76.
[8] A.F. Chudnovskii, Heat Transfer in Dispersed Media, GITTL, Moscow, 1954, Chapter 5 (in Russian).
[9] L.S. Fletcher, Recent developments in contact conductance, J. Heat Transfer ASME 110 (1988) 1059–1069.
[10] G.K. Batchelor, R.W. O'Brien, Thermal or electrical conduction through a granular material, Proc. R. Soc. Lond. A 335 (1977) 313–333.
[11] K.-K. Tio, K.C. Ton, Thermal resistance of two solids in contact through a cylindrical joint, Int. J. Heat Mass Transfer 41 (1988) 2013–2024.
[12] W. Manners, Heat conduction through irregularly spaced plane strip contacts, J. Mech. Eng. Sci. Part C 214 (2000) 1049–1057.

[13] A. Gemant, The thermal conductivity of soils, J. Appl. Phys. 21 (1950) 750–752.
[14] A.V. Gusarov, T. Laoui, L. Froyen, V.I. Titov, Contact thermal conductivity of a powder bed in selective laser sintering, Int. J. Heat Mass Transfer 46 (2003) 1103–1109.
[15] W.W.M. Siu, S.H.-K. Lee, Effective conductivity computation of a packed bed using constriction resistance and contact angle effects, Int. J. Heat Mass Transfer 43 (2000) 3917–3924.
[16] C.K. Chen, C.-L. Tien, Conductance of packed spheres in vacuum, ASME J. Heat Transfer 95 (1973) 302–308.
[17] E.G. Youngs, Steady water flow through unsaturated aggregated porous materials, Transport in Porous Media, submitted for publication.
[18] G.N. Dulnev, V.V. Novikov, Transport Processes in Heterogeneous Media, Energoatomizdat, Leningrad, 1991, pp. 140–147, Chapter 2, (in Russian).
[19] F.G. Avkhadiev, A.R. Kacimov, Analytical solutions and estimations in microlevel flows, J. Porous Media 8 (2005) 1–24.
[20] H.S. Carslaw, J.C. Jaeger, Conduction of Heat in Solids, second ed., Clarenden Press, Oxford, 1959, p. 215.
[21] P.Ya. Polubarinova-Kochina, On the problem of obtaining axisymmetric flows from plane ones, Fluid Dynamics 4 (1969) 133–136 (in Russian).
[22] N.N. Lebedev, Special Functions and Their Applications, Dover, New York, 1972, p. 421.
[23] A.P. Prudnikov, Yu.V. Brychkov, O.I. Marichev, Integrals and Series. V.1. Elementary Functions, V.2. Special Functions, Gordon and Breach, New York, 1986, p. 738.
[24] I.S. Gradshteyn, I. Ryzhik, Tables of Integrals, Series and Products, Academic Press, New York, 1980, p. 41.
[25] P.M. Morse, H. Feshbach, Methods of Theoretical Physics. Pt. II, Pergamon, New York, 1953, pp. 1264–1266.
[26] M.I. Kliot-Dashinskii, Seepage into a small borehole in a confined aquifer with a highly permeable substratum, Izvestiya Akademii Nauk SSSR, Otdelenie Tekhnicheskikh Nauk. (1961) 193–196 (in Russian).
[27] A.K. Das, S.S. Sadhal, Thermal constriction resistance between two solids for random distribution of contacts, Heat Mass Transfer 35 (1999) 101–111.
[28] E.G. Youngs, G. Spoor, G.R. Goodall, Infiltration from surface ponds into soils overlying a very permeable substratum, J. Hydrol. 186 (1996) 327–334.
[29] G. Polya, G. Szego, Isoperimetric Inequalities in Mathematical Physics, Princeton University Press, Princeton, 1951, Section 1.21.
[30] G. Crasta, I. Fragalà, F. Gazzola, On a long-standing conjecture by PolyaSzego and related topics, Zeitschrift fur Angewandte Mathematik und Physik. 56 (2005) 763–782, doi:10.1007/s00033-005-3092-9.
[31] C.K. Ho, S.W. Webb, Review of porous media enhanced vapor-phase diffusion mechanisms, models and data—does enhanced vapor-phase diffusion exist? J. Porous Media 1 (1998) 71–92.
[32] R.A. Fisher, On the capillary forces in an ideal soil; correction of formulae given by Haines, J. Agric. Sci. 16 (1926) 492–505.
[33] A. Sasaki, S. Aiba, H. Fukuda, A study on the thermophysical properties of a soil, ASME J. Heat Transfer. 109 (1987) 232–237.
[34] T. Ochsner, R. Horton, T. Ren, A new perspective on soil thermal properties, Soil Sci. Soc. Am. J. 65 (2001) 1641–1647.